Improving Energy Efficiency for Energy Harvesting Embedded Systems*

Yang Ge, Yukan Zhang and Qinru Qiu
{yage, yzhan158, qiqiu}@syr.edu
EECS department, Syracuse University, New York, 13210, USA

ABSTRACT

While the energy harvesting system (EHS) supplies green energy to the embedded system, it also suffers from uncertainty and large variation in harvesting rate. This constraint can be remedied by using efficient energy storage. Hybrid Electrical Energy Storage (HEES) system is proposed recently as a cost effective approach with high power conversion efficiency and low self-discharge. In this paper, we propose a fast heuristic algorithm to improve the efficiency of charge allocation and replacement in an EHS/HEES equipped embedded system. The goal of our algorithm is to minimize the energy overhead on the DC-DC converter while satisfying the task deadline constraints of the embedded workload and maximizing the energy stored in the HEES system. We first provide an approximated but accurate power consumption model of the DC-DC converter. Based on this model, the optimal operating point of the system can be analytically solved. Integrated with the dynamic reconfiguration of the HEES bank, our algorithm provides energy efficiency improvement and run-time overhead reduction compared to previous approaches.

Keywords

Hybrid electrical energy storage system, energy harvesting system, bank reconfiguration

1. INTRODUCTION

Environmental energy harvesting is a promising technique for sustainable operation of embedded system (e.g. wireless sensor node) and even provides the possibility of unlimited lifetime [1]. However, one of the major constraints of applying energy harvesting technique to real-time embedded system is the uncertainty and large variation in harvesting rate [2]. For a practical implementation of such system, electrical energy storage (EES) element is usually employed to compensate the power fluctuation caused by the energy harvesting. With such an EES element integrated in the system, excessive energy can be stored while the harvesting rate is high. When the harvesting rate is low, the EES element can be a supplement energy source for the embedded system to work properly.

Traditional EES systems are mainly homogenous and have the same type of storage banks. Recently, the Hybrid electrical energy storage system (HEES) [3] has been proposed to overcome the drawbacks of different types of EES banks while exposing their strengths. These EES banks have different characteristics such as cycle efficiency, leakage current, cycle life, storage cost and volumetric energy density, power rating and so on. These EES elements are connected via Charge Transfer Interconnect (CTI) and DC-DC power converters to enable power transfer. Due to the combination of various EES elements, HEES system may show good performance metric including high energy density, high power delivery capacity, low cost, and low leakage.

*This work was partially supported by the National Science Foundation under Grant CNS-0845947.

Several recent research works have addressed different problems in the HEES system. The goal of charge replacement problem [5] is to select which EES banks to be discharged and determine the discharging current of each selected EES bank to support a given load demand. In contrast with drawing power out of the HEES bank, the goal of charge allocation [4] is to solve the dual problem when the external power comes into the HEES system. The goal of charge migration problem [6] is to transfer energy internally from one EES bank to another, while improving the energy efficiency and reducing the energy loss during the transfer process. The HEES system could also be integrated with energy harvesting devices like PV cells [8] to store the maximum amount of solar energy. The main control knobs in these problems are the voltage of charge transfer interconnect V_{cti}, the set of active EES banks and the bank current. The algorithms for finding the optimal control variables in these problems are similar. The outer loop of these algorithms is to select the best V_{cti} for a given active set of EES banks using binary search, while the inner loop is to select the optimal set of active EES banks. In the inner loop, a convex optimization problem is solved iteratively until the set of active banks and the bank terminal voltages converge.

As we can see, one common drawback of these previous works is the high complexity of the algorithm, which might not be feasible for online applications, because the status of the EES banks, the power input to the system and the load characteristics could change rapidly. When these system status change, the control parameters have to be recomputed, which could incur large runtime overhead. Furthermore, other energy optimization techniques, e.g. dynamic voltage frequency scaling (DVFS), EES bank reconfiguration [7], are not considered in these works.

In this paper, we propose a fast heuristic algorithm to improve the energy efficiency for charge allocation and replacement in an EHS/HEES equipped embedded system. We observed that the major energy loss in the system during charge allocation and replacement is on the DC-DC power converters which are important components in the system. So the goal of our algorithm is to minimize the energy overhead on the DC-DC converter while maximizing the energy stored in the HEES system and satisfying the task deadline constraints of the embedded workload. We divide the energy efficiency optimization problem into two parts. When the harvesting power is high enough, the problem becomes charge allocation problem. In addition to supplying the embedded workload, excessive energy will be stored in the HEES system. On the other hand, when the harvesting power is low, the problem becomes charge replacement problem, because the energy is drawn from the HEES to supply the embedded load.

To avoid iteratively solving the complex optimization problem, we first derive a simplified yet accurate power consumption model of the DC-DC converter. We observed that when the input and output voltage of the DC-DC converter matches, the power consumption of the converter is minimized. Therefore, our algorithm tries to match the terminal voltages of the DC-DC converters in the system for both charge allocation and replacement sub-problem. Compare to the previous works

978-1-4673-3030-5/13/$31.00 ©2013 IEEE

[4][5][6][8], in addition to V_{cti} and the active set of banks, our algorithm has one more control knob, i.e. the structure of EES bank. We utilize the EES bank reconfiguration technique to dynamically adjust the connection of the EES bank so that the bank terminal voltage could better match the V_{cti}. For the charge allocation sub-problem, our algorithm set the V_{cti} to match the V_{dd} of the embedded workload. For the charge replacement sub-problem, our algorithm could analytically solve the optimal V_{cti} which minimize the energy wasted on the DC-DC converters.

The following summarizes the key differences between the proposed work and the previous works.

- Unlike the previous works [4][5][6][8], which only consider one sub-problem of the HEES system, our work considers both charge allocation and charge replacement together. In addition to V_{cti} and the active set of banks, the proposed algorithm utilizes the EES bank reconfiguration as additional control knob for better energy efficiency.
- Based on the proposed approximation of the DC-DC power consumption model, our heuristic algorithm has very low complexity compared to the previously proposed algorithms which solve convex optimization problem iteratively and use binary search for optimal V_{CTI}. The simplicity of our algorithm makes it suitable for runtime energy management for systems where the operating conditions vary rapidly.
- Compared to the previous proposed approach, our algorithm can achieve up to 41.23% improvement in energy efficiency for constant power charging and achieve 124.05% improvement in energy efficiency for a system charging and discharging under real solar power profile.

The rest of this paper is organized as follows. The energy harvesting system model and some assumptions are presented in section 2. The proposed heuristic energy management algorithm is described in section 3. Experimental results and discussions are presented in section 4. We conclude our paper in section 5.

2. ARCHITECTURE FOR GREEN POWERED HEES

In this section, we introduce the system architecture of energy harvesting embedded system. Figure 1 shows a block diagram of the system architecture considered in this paper. The system consists of the following components, an energy harvesting system (EHS), several heterogeneous electrical energy storage banks and the embedded systems, i.e. the loads. All these components are connected together through Charge Transfer Interconnect (CTI).

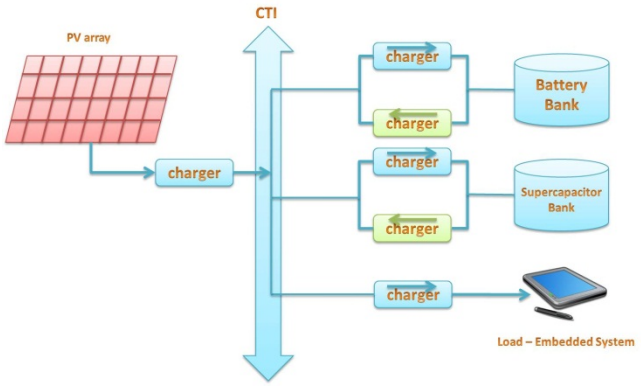

Figure 1 Energy harvesting embedded system architecture

2.1 Energy Harvesting System

On the left part of the system, energy is harvested from the environment by the energy harvesting system and distributed to other components of the system. Although any EHS can be integrated in our system, in this paper, we assume that they are a set of photovoltaic (PV) arrays. The PV array exhibits non-linear current-voltage characteristics so that the output current has to be adjusted dynamically to match the output impedance to draw the maximum amount of power from the PV system. This technique is called maximum power point tracking (MPPT) and there are several methods proposed by previous works that could achieve the MPPT, e.g. the perturb and observe (P&O) method [9], the incremental conduction method [11] and the ripple correlation control method [10]. When the power consumption of the charger is taken into consideration, a maximum power transfer tracking (MPTT) method is proposed [12] to guarantee the maximum amount of power input into the system. In this paper, we assume the MPTT method is applied to the EHS so that the maximum amount of power goes into the system.

2.2 The DC-DC converters

Different components in the system cannot be connected to the charge transfer interconnect directly because these components usually have different operating voltage and current depending on their status. Therefore, the DC-DC power converters are placed between these components and the charge transfer interconnect for voltage and current regulation. A DC-DC converter can provide desired output voltage or current level regardless the status of the storage banks or the loads. In this paper, we assume the converters in the system are all identical uni-directional switching buck-boost converters as shown in Figure 2 [7]. For each EES bank, there are two converters connected to it. One is for charging (charger, blue one) and the other is for discharging (discharger, green one). We assume at any given time, only one converter of these two is on, i.e. the bank is either charging or discharging. When the EES bank is charging, the I_{cti} and I_{bank} are positive while the EES is discharging, they are all negative.

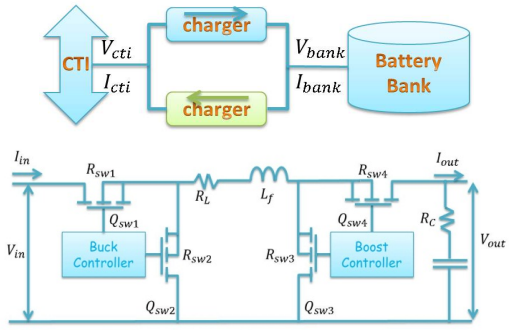

Figure 2 DC-DC power converter structure

When the input voltage V_{in} is larger than the output voltage V_{out}, the DC-DC converter operates at buck mode. On the other hand, when $V_{out} < V_{in}$, the DC-DC converter operates at boost mode. The power consumption P_{dcdc} of the DC-DC converter strongly depends on V_{in}, V_{out} and the output current I_{out}. It consists of three components: conduction loss P_{cdct}, switching loss P_{sw} and controller loss P_{ctrl}. If the DC-DC converter is operating at buck mode, the power components can be expressed as [4]:

$$P_{cdct} = I_{out}^2 \cdot (R_L + D \cdot R_{sw1} + (1-D) \cdot R_{sw2} + R_{sw4}) + \frac{(\Delta I)^2}{12} \cdot (R_L + D \cdot R_{sw1} + (1-D) \cdot R_{sw2} + R_{sw4} + R_c)$$

$$P_{sw} = V_{in} \cdot f_s \cdot (Q_{sw1} + Q_{sw2})$$

$$P_{ctrl} = V_{in} \cdot I_{ctrl}$$

Where $D = V_{out}/V_{in}$ is the duty ratio and $\Delta I = \frac{V_{out} \cdot (1-D)}{L_f \cdot f_s}$ is the maximum current ripple. f_s is the switching frequency; I_{ctrl} is the current flowing into the controller; R_L and R_C are the equivalent series resistance (ESR) of inductor L and capacitor C, respectively; $R_{sw1\ldots4}$ and $Q_{sw1\ldots4}$ are the turn-on resistances and gate charges of the four switches in Figure 2, respectively. The power consumption on the DC-DC converter is the sum of P_{cdct}, P_{sw}, and P_{ctrl}.

If the DC-DC converter is operating at boost mode, the power components can be expressed as:

$$P_{cdct} = \frac{I_{out}^2}{D^2} \cdot (R_L + (1-D) \cdot R_{sw3} + D \cdot R_{sw4} + R_{sw1} + D \cdot (1-D) \cdot R_C) + \frac{(\Delta I)^2}{12} \cdot (R_L + (1-D) \cdot R_{sw3} + D \cdot R_{sw4} + R_{sw1} + D \cdot R_C)$$

$$P_{sw} = V_{out} \cdot f_s \cdot (Q_{sw3} + Q_{sw4})$$

$$P_{ctrl} = V_{in} \cdot I_{ctrl}$$

Where $D = V_{in}/V_{out}$ and $\Delta I = \frac{V_{in} \cdot (1-D)}{L_f \cdot f_s}$.

2.3 Balanced Reconfiguration of HEES Bank

In this paper, we consider two kinds of EES banks, one is supercapacitor bank and the other is battery bank. We assume the storage cells in an EES bank are identical and have same terminal voltages at all time in this paper. As we mentioned, the power consumption of DC-DC converter depends on its input voltage V_{in} and output voltage V_{out}. And we will show in next section, the further apart between V_{in} and V_{out}, the higher P_{dcdc} will be. Therefore, we use EES bank reconfiguration technique to match the V_{in} and V_{out}. Let N be the number of cells in an EES bank, we define that a *balanced configuration* (m, n) of an EES bank has m cells in series and n cells in parallel such that $N = m \times n$. For example, for a four-cell bank, the balanced configurations are $(4,1)$, $(2,2)$ and $(1,4)$. Figure 3 shows the three possible balanced reconfiguration of the four-cell EES bank. Each cell has three switches: one series switch (S-switch, orange one) and two parallel switches (P-switches, green ones) except for the last cell. In the $(4,1)$ configuration, all the S-switches are on while all the P-switches are off. On the other hand, in the $(1,4)$ configuration, only the P-switches are on while all S-switches are off.

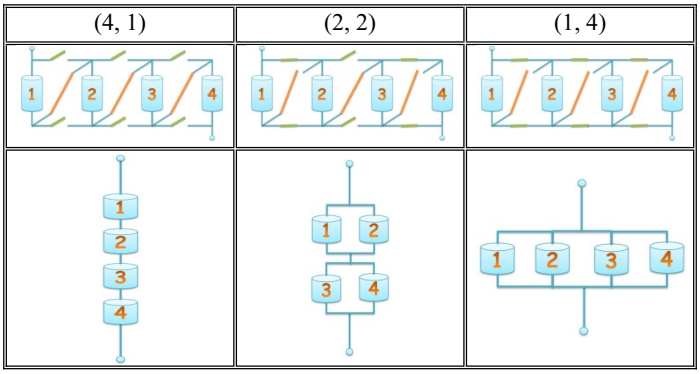

Figure 3 Reconfiguration of an EES bank

3. EFFICIENT HEURISTIC ENERGE MANAGEMENT ALGORITHM

3.1 Problem Formulation

For an energy harvesting embedded system modeled in the last section, energy is harvested from the renewable source and is either consumed immediately by the embedded system (load) or stored in the HEES bank for future use. As the energy flow through the system, some portion of the energy inevitably lost in the system. The major loss in such a system is caused by the energy consumption of the DC-DC converters. Therefore, to improve the energy efficiency of the whole system, we have to reduce the energy wasted on the DC-DC converters.

In such a system, there are several control knobs we could manipulate to achieve the energy efficiency. For example, the voltage of the CTI V_{cti}, the configuration of the HEES bank and operating conditions of the embedded system. We formally define our problem as following.

Given: the harvesting power profile $G(t)$, the load application characteristics.

Goal: dynamically adjust the V_{cti}, the configuration of the HEES bank and the operating voltage and current of the embedded system such that the energy wasted on the DC-DC converters is minimized and the energy stored in the HEES bank is maximized. And the deadline of the embedded application is satisfied.

3.2 Approximation of the Power Consumption of the DC-DC Converter

The above equation shows that the power consumption of the DC-DC converter P_{dcdc} is a function depends on the input voltage V_{in}, output voltage V_{out} and output current I_{out}. And the P_{dcdc} consists of three parts P_{cdct}, P_{sw} and P_{ctrl}. We further divided the P_{cdct} into two parts: P_{cdct1} and P_{cdct2}.

For buck mode:

$$P_{cdct1} = I_{out}^2 \cdot (R_L + D \cdot R_{sw1} + (1-D) \cdot R_{sw2} + R_{sw4})$$

$$P_{cdct2} = \frac{(\Delta I)^2}{12} \cdot (R_L + D \cdot R_{sw1} + (1-D) \cdot R_{sw2} + R_{sw4} + R_c)$$

For boost mode:

$$P_{cdct1} = \frac{I_{out}^2}{D^2} \cdot (R_L + (1-D) \cdot R_{sw3} + D \cdot R_{sw4} + R_{sw1} + D \cdot (1-D) \cdot R_C)$$

$$P_{cdct2} = \frac{(\Delta I)^2}{12} \cdot (R_L + (1-D) \cdot R_{sw3} + D \cdot R_{sw4} + R_{sw1} + D \cdot R_C)$$

Because the resistance R_{sw1} and R_{sw2}, R_{sw3} and R_{sw4} have about the same value, we can simplify P_{cdct1} and P_{cdct2} as the following.

For buck mode:

$$P_{cdct1} = I_{out}^2 \cdot (R_L + R_{sw1} + R_{sw4})$$

$$P_{cdct2} = \frac{(\Delta I)^2}{12} \cdot (R_L + R_{sw1} + R_{sw4} + R_c)$$

For boost mode:

$$P_{cdct1} = \frac{I_{out}^2}{D^2} \cdot (R_L + R_{sw4} + R_{sw1} + D \cdot (1-D) \cdot R_C)$$

$$P_{cdct2} = \frac{(\Delta I)^2}{12} \cdot (R_L + R_{sw4} + R_{sw1} + D \cdot R_C)$$

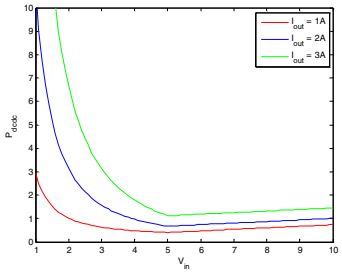

Figure 4 P_{dcdc} against V_{in} curve

As we can see, the power component P_{sw} and P_{ctrl} are linearly dependent on V_{in} and V_{out} in buck and boost mode respectively. P_{cdct1} is a constant in buck mode when I_{out} is fixed and a non-linear function of V_{in} and V_{out} in boost mode. P_{cdct2} is a non-linear functions of both V_{in} and V_{out}. To illustrate the relation between the DC-DC power consumption and the related variables, we fix the $V_{out} = 5V$ and plot the P_{dcdc} against V_{in} for I_{out} is 1A (red), 2A (blue) and 3A (green) in Figure 4.

As shown in the figure that when the DC-DC converter is operating at buck mode, i.e. $V_{in} > V_{out}$, the P_{dcdc} increases almost linearly against the V_{in}, which means the linear part is dominant in this region. Furthermore, we observe that when $V_{in} = V_{out}, P_{cdct2} = 0$; when $V_{in} \to \infty$, $P_{cdct2}$is a constant. In both cases, P_{cdct2} is is much smaller than P_{cdct1}. Therefore we could safely omit the non-linear part P_{cdct2}. Now P_{dcdc} only linearly depends on V_{in} and I_{out}^2 as following

$$P_{dcdc} = P_{cdct1} + P_{sw} + P_{ctrl} = I_{out}^2 \cdot (R_L + R_{sw1} + R_{sw4}) + V_{in} \cdot f_s \cdot (Q_{sw1} + Q_{sw2}) + V_{in} \cdot I_{ctrl} \quad (1)$$

On the other hand, when the converter is operating at boost mode, i.e. $V_{in} \le V_{out}$, the power consumption increases non-linearly as the V_{in} decreases, which means that the non-linear parts (i.e. P_{cdct1} and P_{cdct2}) are dominant in this region. In boost mode, when $V_{in} = V_{out}$, P_{cdct2} is 0 while P_{cdct1} is non-zero. As $V_{in} \to 0$, $D \to 1$, so $P_{cdcd1} \to \infty$, and P_{dcdc2} is a finite number. This suggests that P_{dcdc2} can again be omitted compared to P_{cdcd1}. Therefore, we approximate the P_{dcdc} in boost mode as following.

$$P_{dcdc} = P_{cdct1} + P_{sw} + P_{ctrl} = \left(\frac{I_{out}V_{out}}{V_{in}}\right)^2 \cdot (R_L + R_{sw4} + R_{sw1}) + V_{out} \cdot f_s \cdot (Q_{sw3} + Q_{sw4}) + V_{in} \cdot I_{ctrl} \quad (2)$$

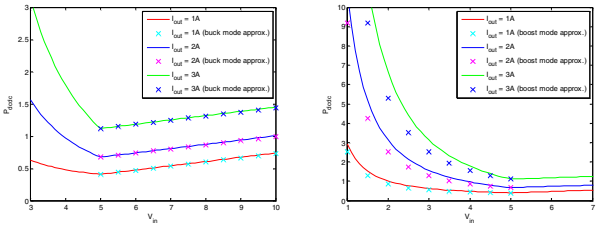

Figure 5 Fitting results of our approximation

Figure 5 compares the simplified P_{dcdc}(i.e. Equation (1)) and its original function given in Section 2.2. It shows that the approximation closely follows the original function.

We have several observations based on the above analysis. Firstly, for the given V_{out} and I_{out}, P_{dcdc} reaches its minimum at $V_{in} = V_{out}$. Secondly, as the V_{in} moves away from V_{out}, P_{dcdc} increases much faster in the boost mode than in the buck mode. These two observations suggest that it is better to operate the DC-DC converter at buck mode and set the V_{in} close to V_{out}. Thirdly, P_{dcdc} increases as the I_{out} increases.

3.3 The Optimal V_{cti} for Discharging

Given the load power consumption characteristics and current status of one energy storage bank, we are interested in finding the optimal V_{cti} to maximize the discharging efficiency, i.e. to minimize the power consumption on the two DC-DC converters, (dcdc1 connects the bank and the CTI and dcdc2 connects the CTI and the load). Based on the approximation of P_{dcdc} in the last section, we can derive an analytic expression for the optimal V_{cti} in discharging process. Assume both the converters are operating in the buck mode, the operating voltage and current for the load is V_{load} and I_{load}, and the EES bank voltage is V_{bank}. Then the power consumption of the two DC-DC converters are given as

$$P_{dcdc1} = \alpha V_{bank} + \beta I_{cti}^2$$
$$P_{dcdc2} = \alpha V_{cti} + \beta I_{load}^2$$

We could substitute the I_{cti} with $(P_{dcdc2} + P_{load})/V_{cti}$, because the power provided by the CTI is consumed by the load and dcdc2. Our goal is to find the best V_{cti} to minimize $P_{dcdc} = P_{dcdc1} + P_{dcdc2}$. We differentiate P_{dcdc} with the variable V_{cti} and set it to 0 as following

$$\frac{\partial P_{dcdc}}{\partial V_{cti}} = \alpha - \frac{2\alpha\beta\gamma}{V_{cti}^2} - \frac{2\alpha\gamma^2}{V_{cti}^3} = 0$$

i.e.

$$V_{cti}^3 - 2\beta\gamma V_{cti} - 2\gamma^2 = 0$$

In the above equation, $\gamma = \beta I_{load}^2 + P_{load}$. Because it is a cubic equation, it is analytically solvable [13], and we could find the optimal V_{cti} by solving the above equation. Let V_{opt} denote the optimal V_{cti} , one observation that can be made from the above analysis is that the value of V_{opt} is only determined by the load characteristics and does not depend on the status of the bank V_{bank}, as long as V_{bank} is high enough to make both DC-DC converters operates at the buck mode. However the P_{dcdc} does increase as the V_{bank} increase. This also suggests that we should set the V_{bank} to be the lowest level that is greater than V_{opt}. This provides a guideline for the reconfiguration of the HEES banks.

3.4 Efficient Energy Management Algorithm

In this section, we describe our efficient energy management algorithm. Our algorithm can be divided into two parts. The first part is called charging process, which is used when the harvesting power is high (e.g. during the noon) and in addition to supplying the load, there is extra energy that can be stored in the HEES bank. The second part is called discharging process which is used when harvesting power is low or even zero, e.g. in the early morning or during the midnight. In this case, energy has to be drawn from the HEES system.

The main idea of our algorithm is to save the energy wasted on DC-DC converter to improve the energy efficiency by dynamically adjusting the operating voltage and frequency of the load, the voltage of interconnect V_{cti} and the configuration of the HEES system. We use one bank from the HEES system as the source for charging or discharging at a time so that only one DC-DC converter will be turned on, therefore the energy consumed by DC-DC converter can be reduced. We use the supercapacitor banks as the primary charging/discharging source while leaving the battery bank as the secondary source because supercapacitors have very high cycle efficiency and bigger voltage swings than the batteries so that the input and output voltage of the DC-DC convert can be matched better. In addition, the supercapacitor has no rate capacity effects as the battery.

We summarize our charging process in Algorithm1. For a given workload, we first find the optimal V_{load} and I_{load} to minimize the energy consumption of the embedded application. Any existing optimization algorithm can be integrated because this step is independent with other parts of the algorithm. If the supercapacitor bank is not fully charged, we will charge the supercapacitor bank, otherwise we will charge the battery bank.

As we show in section 3.2, the P_{dcdc} is minimized when V_{in} matches V_{out}, and buck mode is more energy efficient than boost mode. So the ideal charging situation would be $V_{cti} = V_{load} = V_{bank}$. But this might not always be possible depending on the amount of energy stored in the HEES bank. Therefore, we select a configuration that gives the highest bank voltage $V_{bank,cap}$ that is smaller than V_{load} (line 3). In this case, if we set $V_{cti} = V_{load}$, one

converter is operating at buck mode and another converter's input voltage and output voltage are same. Therefore the energy on DC-DC converters is reduced. However, if we are not able to find a configuration with $V_{bank,cap}$ less than V_{load}, then we will set all capacitors connecting in parallel to reduce the bank terminal voltage and set $V_{cti} = V_{bank,cap}$. In this case, the DC-DC converter on the supercapacitor bank side (i.e. dcdc1) has matching input and output voltage while the converter on the load side (i.e. dcdc2) operating at buck mode (line 6). If the supercapacitor bank is fully charged, we will charge the battery bank. The configuration for battery bank (line 8~11) is similar as the configuration for supercapacitor bank (line 3~6).

Algorithm 1: Charging Process

1. Find the most energy efficient V_{load} and I_{load} setting for current load
2. **if** (supercapacitor bank is not full) // Charge the supcap bank
3. (s,p) = Choose a config. s.t. $V_{bank,cap} \leq V_{load}$ and V_{bank} is closet to V_{load}
4. **if** $((s,p) == \emptyset)$
5. $(s,p) = (1, N_{cap})$
6. $V_{cti} = \max(V_{bank,cap}, V_{load})$
7. **else** // Charge the battery bank
8. (s,p) = Choose a config. s.t. $V_{bank,bat} \leq V_{load}$ and V_{bank} is closet to V_{load}
9. **if** $((s,p) == \emptyset)$
10. $(s,p) = (1, N_{bat})$
11. $V_{cti} = \max(V_{bank,bat}, V_{load})$
12. **return** V_{cti}, (s,p);

The discharging process is shown in algorithm 2. Again, we first find the optimal V_{load} and I_{load} that minimize the energy consumption of the embedded application. Next, we use the method discussed in section 3.3 to find the optimal CTI voltage V_{opt} and set $V_{cti} = V_{opt}$ (line 2). Then we will discharge from the supercapacitor bank if it is not empty. From the discussion in section 3.3, it is better to operate the DC-DC converter at lower input voltage for energy efficiency as long as it is in buck mode. Therefore, we select a configuration such that gives the lowest bank terminal voltage $V_{bank,cap} \geq V_{opt}$ (line 4). If there is no such feasible configuration, we will connect all supercapacitors in series. We will switch to battery bank for discharging until the supercapacitor bank is depleted. The configuration process for battery bank (line 8~10) is similar as that of supercapacitor bank (line 4~6).

Algorithm 2: Discharging Process

1. Find the most energy efficient V_{load} and I_{load} setting for current load
2. Find the optimal CTI voltage V_{opt} for (V_{load}, I_{load}), set $V_{cti} = V_{opt}$
3. **if** (supercapacitor bank is not empty) // Discharge from supcap bank
4. (s,p) = Choose a config. s.t. $V_{bank,cap} \geq V_{opt}$ and $V_{bank,cap}$ is closet to V_{opt}
5. **if** $((s,p) == \emptyset)$
6. $(s,p) = (N_{cap}, 1)$
7. **else** // Discharge from the battery bank
8. (s,p) = Choose a config. s.t. $V_{bank,bat} \geq V_{opt}$ and $V_{bank,bat}$ is closet to V_{opt}
9. **if** $((s,p) == \emptyset)$
10. $(s,p) = (N_{bat}, 1)$
11. **return** V_{cti}, (s,p);

4. Experimental Results

To demonstrate the effectiveness of the proposed algorithm, we implement a C++ simulator to model the HEES system. The HEES consists of one supercapacitor bank and one battery bank. The supercapacitor bank consists of 4 capacitors with 100F capacitance [7][8]. We obtain other components like battery and DC-DC power converter model parameters from [14]. These parameters are obtained from the datasheets of the real devices. We assume the load power consumption is constant for a given period.

4.1 Constant Input Power Results

In this section, we compare the energy efficiency of our heuristic algorithm and that of the algorithm proposed in previous works [4][5][6][8]. The previous work is referred as *Adaptive* V_{cti}. As mentioned before, this algorithm uses binary search to adaptively adjust V_{cti} to minimize the energy consumed on the DC-DC converters. It does not consider the reconfiguration of the HEES.

Table 1 Energy stored in HEES for constant power input

Configuration	(4, 1) (J)	(2, 2) (J)	(1, 4) (J)	Our (J)
1.75w	169.92	189.75	179.67	194.75
1.25w	15.05	14.77	13.49	19.05

Table 1 shows the amount of energy stored in the HEES system after it is charged using constant power input for 10 minutes. In this set of experiments, because there are 4 supercapacitors in the supercapacitor bank, the possible configurations of the bank are $(4,1)$, $(2,2)$ and $(1,4)$ as shown in the example of section 2.3. We consider two scenarios when the input power to the system is 1.75w and 1.25w. In the former case, our heuristic algorithm stores 14.61%, 2.64% and 8.39% more energy compared to the Adaptive V_{cti} algorithms whose potential configurations are $(4,1)$, $(2,2)$ and $(1,4)$ respectively. While in the latter case, the proposed algorithm stores 26.58%, 28.96% and 41.23% more energy. As we could see, one supercapacitor configuration might work better than others at certain power input level, when the power input level changes, their efficiency will degrade. However, our algorithm works consistently better than the fixed configuration. Although the *Adaptive* V_{cti} algorithm always finds the optimal V_{cti} for a fixed configuration, it can still produce large imbalance between the input and output voltage of the DC-DC converters. Therefore it cannot minimize the power consumed on the converters. On the contrary, through reconfiguration, our algorithm can always keep the terminal voltage of the DC-DC converters better matched. Thus it is more effective in reducing the energy wasted on the converters.

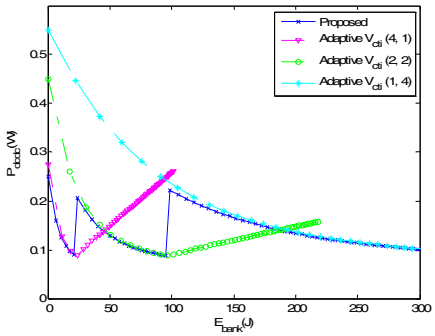

Figure 6 P_{waste} against the energy stored in the EES bank

Figure 6 further explains why our algorithm can improve energy efficiency. This figure shows the wasted power against the energy stored in the supercapacitor bank during the charging process. Wasted power consists of the power consumed on the DC-DC converter and on the internal resistance of the EES bank. Apparently, when the EES bank does not store too much energy, it is better to connect them in series (i.e. (4, 1) configuration) to produce higher terminal voltage so that input and output voltage of the DC-DC converter can be better matched. As the charging process continues, the bank energy as well as the terminal voltage increases, the (4, 1) configuration first enters the boost mode, and

the P_{waste} starts to increase. In this time, it is better to reconfigure the bank to (2, 2). Overall, our algorithm is able to track the most energy efficient bank configuration during the charging process.

Our algorithm could achieve better energy efficiency during discharge process as well. In the second set of experiment, we start using the energy stored in the HEES system to provide the load demands after the 10 minutes charging mentioned before. Our algorithm could last 17.24%, 4.11% and 32.59% longer compared to Adaptive V_{CTI} with (4,1), (2,2) and (1,4) configurations respectively when the input power is 1.75W, and last 23.15%, 44.57% and 72.73% longer when in 1.25W.

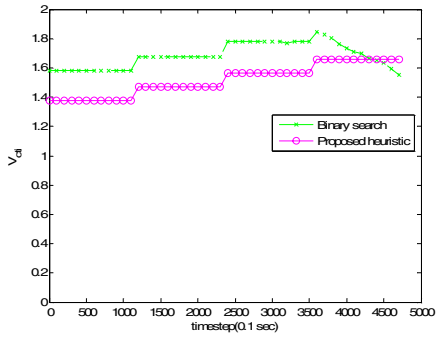

Figure 7 V_{cti} comparison between our proposed heuristic and binary search

Figure 7 shows the comparison of V_{cti} change between the base line *Adaptive* V_{cti} approach and our approach based on the approximation mode during the discharge process. In this experiment, we fix the bank configurations of both approaches to be $(4, 1)$. And the load changes from 1.0w to 1.3w with a period of 120 seconds. The *Adaptive* V_{cti} policy uses binary search method to find the V_{cti} which minimizes the energy wasted on DC-DC converters. Although the V_{cti} is optimal, the searching process is time consuming and might not be applicable in time critical applications. Based on our approximation of the DC-DC converter power model, V_{cti} can be computed directly. As the figure shows, our method tracks the optimal V_{cti} pretty well.

4.2 Variable Sun Power Charging System

Table 2 Energy stored in HEES for real solar irradiation

Config.	(4, 1) (J)	(2, 2) (J)	(1, 4) (J)	Our (J)
Energy	325.504	558.459	711.643	729.287
Impr.	124.05%	30.59%	2.48%	

In this section, we integrated a real solar irradiation profile [12] as the power input to our system. We start charging the system from 11:00am to 12:00pm when the solar irradiance reaches its maximum value. As Table 2 shows, in this charging profile, our algorithm outperforms the baseline algorithm with previously mentioned three configurations by 124.05%, 30.59% and 2.48% respectively. During the charging process, the bank terminal voltages of configuration (4, 1) and (2, 2) exceeds the input voltage of the DC-DC converters for a long time, which means they spend a large portion of time in boost mode which has low energy efficiency. As a result, large amount of energy wasted on DC-DC converters and less amount of energy is stored in the HEES bank for future use. We again compare the discharging time after this charging process. The proposed algorithm last 140.22%, 34.02% and 5.29% longer compared to (4, 1), (2, 2) and (1, 4) configuration respectively.

5. CONCLUSIONS

In this paper, we proposed an efficient heuristic algorithm for the energy efficiency optimization problem of charge allocation and replacement in an EHS/HEES equipped embedded system. Our goal is to minimize the energy wasted on the DC-DC converters while maximizing the energy stored in the HEES system. To avoid the complexity of iteratively searching the optimal operating point, we developed an approximation power model of the DC-DC converter. Based on this model, our algorithm tries to match the input and output voltages of the DC-DC converters by dynamically adjusting the V_{dd} of the embedded load, the charge transfer interconnect voltage V_{cti} and the storage bank terminal voltage using reconfiguration. Experimental results show that our algorithm could store up to 124.05% more energy during charging process and last up to 140.22% longer during discharging process.

6. REFERENCES

[1] V. Raghunathan, A. Kansal, J. Hsu, J. Friedman and Mani Srivastava, "Design considerations for solar energy harvesting wireless embedded systems," In *Proc. of the 4th intern. Symp. on Information processing in sensor networks* (IPSN '05), 2005.

[2] S. Liu, Q. Wu and Qinru Qiu, "An Adaptive Scheduling and Voltage/Frequency Selection Algorithm for Real-time Energy Harvesting Systems," in *Proc. of Design Automation Conference* (*DAC*), July 2009.

[3] M. Pedram, N. Chang, Y. Kim and Y. Wang, "Hybrid electrical energy storage systems," in *Proc. of International Symposium on Low Power Electronics and Design,* Aug. 2010, pp. 363-368.

[4] Q. Xie, Y. Wang, Y. Kim, N. Chang and M. Pedram, "Charge allocation for hybrid electrical energy storage systems," in *Proc. of CODE+ISSS,* Oct. 2011.

[5] Q. Xie, Y. Wang, M. Pedram, Y. Kim, D. Shin and N. Chang, "Charge replacement in hybrid electrical energy storage systems," in *Proc. of Asia and South Pacific Design Automation Conference,* Jan. 2012.

[6] Y. Wang, Y. Kim, Q. Xie, N. Chang, and M. Pedram, "Charge migration efficiency optimization in hybrid electrical energy storage (HEES) systems," in *Proc. of the Int'l Symposium on Low Power Electronics and Design,* Aug. 2011.

[7] Y. Kim, S. Park, Y. Wang, Q. Xie, N. Chang, M. Poncino, and M. Pedram, "Balanced reconfiguration of storage banks in a hybrid electrical energy storage system," *Proc. of Int'l Conference on Computer Aided Design,* Nov. 2011.

[8] Y. Wang, X. Lin, Y. Kim, N. Chang, and M. Pedram, "Enhancing Efficiency and Robustness of a Photovoltaic Power System Under Partial Shading," in *Proc. of the 13th Int'l Symposium on Quality of Electronic Design,* Mar. 2012.

[9] D. Hohm and M. Ropp, "Comparative study of maximum power point tracking algorithms using an experimental, programmable, maximum power point tracking test bed," in IEEE PSC, 2000.

[10] T. Esram, J. Kimball, P. Krein, P. Chapman, and P. Midya, "Dynamic maximum power point tracking of photovoltaic arrays using ripple correlation control," IEEE T. on Power Electonics, 2006.

[11] F. Liu, S. Duan, F. Liu, B. Liu, and Y. Kang, "Avariable step size INC MPPT method for PV systems,"IEEE T. on Industrial Electron., 2008.

[12] Y. Kim, N. Chang, Y. Wang, and M. Pedram, "Maximum power transfer tracking for a photovoltaic-supercapacitor energy system," in *Proc. of Symposium on Low Power Electronics and Design,* Aug. 2010, pp. 307-312.

[13] Nathan Jacobson, *Basic algebra*, vol. 1 (2nd ed.), Dover, 2009.

[14] D. Shin, Y. Wang, N. Chang, and M. Pedram, "Battery-super-capacitor hybrid system for high-rate pulsed load applications," in *Proc. of Design Automation and Test in Europe,* Mar. 2011.